Tracking the mind's image in the brain I: Timeresolved fMRI during visuospatial mental imagery.

Neuron, Vol. 35, 185–194, July 3, 2002, Copyright ©2002 by Cell Press

Tracking the Mind's Image in the Brain I: Time-Resolved fMRI during Visuospatial Mental Imagery

Elia Formisano,[1] David E.J. Linden,[2,3] Francesco Di Salle,[4,8] Luigi Trojano,[5] Fabrizio Esposito,[6] Alexander T. Sack,[3] Dario Grossi,[7] Friedhelm E. Zanella,[4] and Rainer Goebel[1,9]

[1]Department of Cognitive Neuroscience
Faculty of Psychology
Universiteit Maastricht
Postbus 616
6200MD Maastricht
The Netherlands

[2]Max-Planck-Institut für Hirnforschung
Deutschordenstrasse 46
60528 Frankfurt am Main
Germany

[3]Department of Psychiatry
Laboratory for Neuroimaging and Neurophysiology

[4]Department of Neuroradiology
Klinikum der Johann Wolfgang Goethe-Universität
Theodor-Stern-Kai 7
60590 Frankfurt am Main
Germany

[5]Salvatore Maugeri Foundation
IRCCS
Center of Telese
Loc. S. Stefano in Lanterria
82037 Telese Terme (BN)
Italy

[6]Institute of Neurological Sciences
Second University of Naples
Piazza Luigi Miraglia
80138 Naples
Italy

[7]Department of Psychology
Second University of Naples
Via Vivaldi 43
Caserta
Italy

[8]Department of Neuroradiology
Federico II University
Nuovo Policlinico
Via S. Pansini 5
80131 Naples
Italy

Summary

Mental imagery, the generation and manipulation of mental representations in the absence of sensory stimulation, is a core element of numerous cognitive processes. We investigate the cortical mechanisms underlying imagery and spatial analysis in the visual domain using event-related functional magnetic resonance imaging during the mental clock task. The time-resolved analysis of cortical activation from auditory perception to motor response reveals a sequential activation of the left and right posterior parietal cortex, suggesting that these regions perform distinct functions in this imagery task. This is confirmed by a trial-by-trial analysis of correlations between reaction time and onset, width, and amplitude of the hemodynamic response. These findings pose neurophysiological constraints on cognitive models of mental imagery.

[9]Correspondence: r.goebel@psychology.unimaas.nl

Introduction

The cognitive processes required to generate mental images and to analyze them are subserved by a distributed network of brain regions. Traditionally, the attempt to dissect these processes into a sequence of processing stages has been based on the analysis of reaction times (mental chronometry) (Posner, 1978; Shepard and Cooper, 1982; Kosslyn, 1994). The temporal information provided by mental chronometry could be complemented by information about the spatiotemporal pattern of cortical activation obtained by physiological methods, such as event-related potentials (Renault et al., 1982; Hillyard, 1993) and, more recently, magnetoencephalography (Raij, 1999) and event-related functional magnetic resonance imaging (fMRI) (Menon and Kim, 1999). This last method has been used to relate the behavioral data of visual and visuomotor tasks to the latency and duration of the blood oxygen level-dependent (BOLD) response in restricted brain regions (Menon et al., 1998; Richter et al., 2000). We employed this technique in order to address the question of functional differentiation between the various cortical areas involved in a complex cognitive task, the mental clock task (Paivio, 1978; Grossi et al., 1989).

In this task, subjects are asked to imagine pairs of clock faces on the basis of acoustically presented times, to compare the mental images, and to report in which of the two faces the clock hands form the greater angle. The mental clock task thus involves auditory perception, the translation of the auditory information into mental representations that preserve the angular differences, the comparison of the angles, and a behavioral response. The mental clock task requires several seconds of processing which allowed us to track its traces in the brain with event-related fMRI.

During fMRI measurements, pairs of times were presented every 16 s (e.g., "nine thirty, eight o'clock...."). Subjects were instructed to imagine the corresponding analog clock faces and push a button with their index finger if the hands of the first clock formed the greater acute angle or another button with their middle finger if the hands of the second clock formed the greater acute angle. A high resolution ($1 \times 1 \times 1$ mm^3) anatomical data set covering the whole brain of the subject was collected during the same scanning session and was used for the reconstruction of the cortical surface. After preprocessing and coregistration with anatomical images, functional time series were analyzed using both multi- and single-subject multiple regression analysis (Friston et al., 1995). Three predictors, defined to repre-

Table 1. Behavioral Results

Side of Imagined Clock Hands	Response Hand	Correct Reaction Times [ms] (Mean ± SEM)	Percent Correct Responses (Mean ± SEM)
Right	Right	2859 ± 142	96.4 ± 0.02
Right	Left	2512 ± 115	96.9 ± 0.03
Left	Right	3152 ± 150	91.1 ± 0.02
Left	Left	2770 ± 133	95.8 ± 0.03

For each subject ($n_1 = 6$), the mean reaction time for correct responses and the percentage of correct responses were computed for each of the four conditions defined by the combination of side of imagined clock hands and response hand. A 2 × 2 analysis of variance for repeated measures, with hand (right versus left) and side (right versus left half of the clock face) as within-subjects factors, was applied to mean correct reaction times and to percentage of correct responses. The total number of correct responses was 363/384. The analysis showed significant effects of the side of imagined clock hands ($F[1,5] = 14.54$; $p = 0.012$) and the hand of button press response ($F[1,5] = 11.49$, $p = 0.019$) and a nonsignificant side-hand interaction ($F[1,5] < 1$, $p = 0.9$). No significant effect were found for percentage of correct responses.

sent the auditory instruction, the mental imagery, and the motor response, were used to build the design matrix of the experiment. For significantly activated voxels, the latency of the estimated hemodynamic response (HR) was color coded with a blue-green-yellow-red scale and visualized through projection on inflated and flattened representations of the cortical sheet of a template brain (group map) or of the subject's brain (individual maps, see Experimental Procedures). Moreover, for all the cortical regions that were activated during the task, we performed a trial-by-trial analysis of the HRs that allowed us to establish a link between behavior, as measured by RT, and brain activity, at the spatial and temporal scale of fMRI.

Because latency differences of evoked HRs in different brain areas can have many non-neuronal biophysical causes, the interpretation of these results will require particular caution. However, in our report, we focus on latency differences in homologous regions in the two hemispheres. In this situation, we can assume that the hemodynamic responses are going to be at least comparable. More importantly, by looking at the dependence of onset latency and duration of evoked responses on the reaction time, trial by trial, we restrict our inferences about chronometry to a single region. In this context, we know that the biophysical parameters are the same and any timing differences must be attributable to underlying neuronal dynamics.

Results

Behavioral Results

Subjects correctly identified the greater angle on 95% of the trials with an average reaction time of 2832 ms. Trials were balanced for the response hand (left or right) and the side in which the imagined clock hands were located assuming that the clock face was centered on fixation. Subjects responded significantly faster when the imagined clock hands were in the right visual hemifield and when they used their left hand (Table 1). Neither hemifield nor response hand had a significant effect on response accuracy.

fMRI Results

Group Results

The statistical map of brain activation as detected with the multiple regression analysis of the group data is shown in Figure 1. The relative latency of the hemodynamic response is shown color coded on an inflated and flattened representation of a template brain. Early BOLD activation (blue) was observed in the auditory cortex (transverse temporal gyrus) and along the superior temporal sulcus bilaterally. The dorsolateral prefrontal cortex (DLPFC) and regions in the posterior parietal cortex (PPC) (mainly the intraparietal sulcus [IPS] region in the left hemisphere) became active slightly later (blue-green). Activation proceeded to the supplementary motor area (SMA) (green) and the right PPC (IPS region, extending medially to the sulcus) (green-yellow). The last regions to be activated were the inferior frontal gyrus (yellow), the frontal eye fields (FEF) at the posterior end of the superior frontal sulcus, and the sensorimotor cortex bilaterally (yellow-red).

The time courses of the BOLD responses of the activated regions, averaged across subjects ($n_1 = 6$, repetition time [TR] = 2s) and across trials, are shown in Figure 2A. The signal in the auditory cortex rose from the baseline at a latency (measured from the stimulus onset) of 2 s and reached its peak at 8 s. This signal reflects the auditory cortex activation during the stimulus presentation. The onset of the activation of the bilateral sensorimotor cortex occurred 3–4 s later, corresponding approximately to the average reaction time. The frontal and parietal regions peaked in between, reflecting intermediate levels of processing between the (early) sensory and the (late) motor components of the task (Figure 2A). The group statistics showed a significant difference ($p = 0.002$, corrected) between the relative latency of the time course of the left (1.28 ± 0.39 s) and the right (3.21 ± 0.27 s) PPC (Figure 2B, Table 2). In all the other regions identified bilaterally in the statistical map, the latency of the BOLD response of the left and the right hemispheres did not show any significant difference (Table 2).

This spatio-temporal pattern of brain activation during the mental clock task was confirmed in a second group of six subjects, in which functional time series were collected at a coarser spatial resolution but at a higher temporal resolution (TR = 1.3 s).

Figures 2C and 2D show the time courses of the BOLD responses of the auditory cortex, the left and right PPC, and the motor cortex, averaged respectively across the subjects of this second group that used the right ($n_{2R} = 3$, Figure 2C) or the left hand ($n_{2L} = 3$, Figure 2D) for the

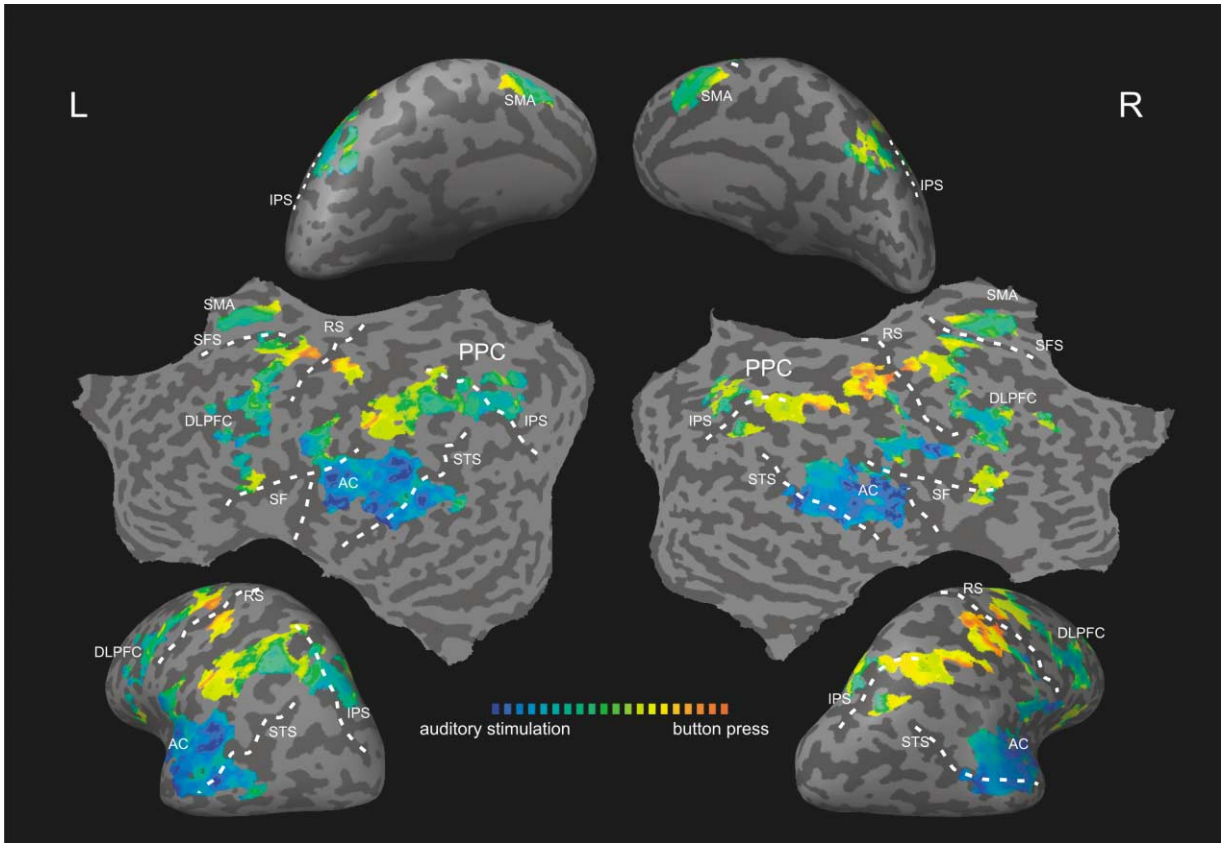

Figure 1. Cortex-Based Multiple Regression Analysis of fMRI Time Series: Group Results

Multi-subject ($n_1 = 6$) general linear model surface map superimposed on flattened and inflated (top—medial view; bottom—lateral view) representations of the cortical sheet of a template brain normalized in Talairach space.

The color of significantly task-related voxels ($p < 0.001$, corrected) encodes the latency of BOLD activation following the auditory presentation of the stimulus. Blue (red) color indicates early (late) latencies of task-related activation corresponding to the auditory stimulation (motor response). Intermediate latencies of task-related activation are linearly represented according to the color bar.

IPS = intraparietal sulcus (posterior branch), PPC = posterior parietal cortex, STS = superior temporal sulcus, AC = auditory cortex, RS = rolandic sulcus, SMA = supplementary motor cortex, SF = Sylvian fissure, SFS = superior frontal sulcus, DLPFC = dorso-lateral prefrontal cortex.

button press (see Figure 2 in Sack et al., 2002 [this issue of *Neuron*] for the corresponding statistical maps).

Individual Results

Figure 3 shows the results of the cortex-based multiple regression analysis of individual fMRI time series in a case of button press response with the right (A) and with the left (B) hand. The relative latency of the hemodynamic response is shown color coded on the flattened representation of the subject's cortex (see Experimental Procedures). The single-subject analysis confirmed the topography and sequence of activation of the brain regions that were obtained with the multi-subject analysis (see Figure 1). Indeed, the spatio-temporal layout of the individual cortical surface maps reflected the sequential activation of the transverse temporal gyrus and of the superior temporal sulcus bilaterally (blue color in Figure 3), the fronto-parietal regions, the anterior SMA (blue-green-yellow colors in Figure 3), and the sensorimotor cortex contra and, to a lesser extent, ipsilateral to the response hand (red color in Figure 3). For some functional runs, however, the clusters of activation in the DLPFC, FEF, and inferior frontal gyrus, which are visible in the group analysis, could not be detected at the selected conservative threshold. Conversely, in some cases, small clusters of activation in a more posterior region of the SMA, showing roughly the same latency as the sensorimotor cortex, were more clearly visible in the individual than in the group analysis.

Both in the cases of response with the right hand and of response with the left, the spatio-temporal pattern of activation in the fronto-parietal regions presented very typical features. Clusters with early activation (blue-green colors in Figure 3) were located mainly, but not exclusively, in the left PPC. Additional clusters with similar activation latency were also present in the right PPC (Figures 3A and 3B) and, in some cases, in the DLPFC (Figure 3A). Clusters with late activation were almost exclusively located in the right PPC (yellow colors in Figure 3) along the superior part of the IPS. Although the activation in the right PPC often extended to a more medial region of the IPS, the temporal shift between the hemodynamic responses in the left and right PPC could be observed even when symmetric anatomical locations were selected (see inserts in Figure 3). No significant

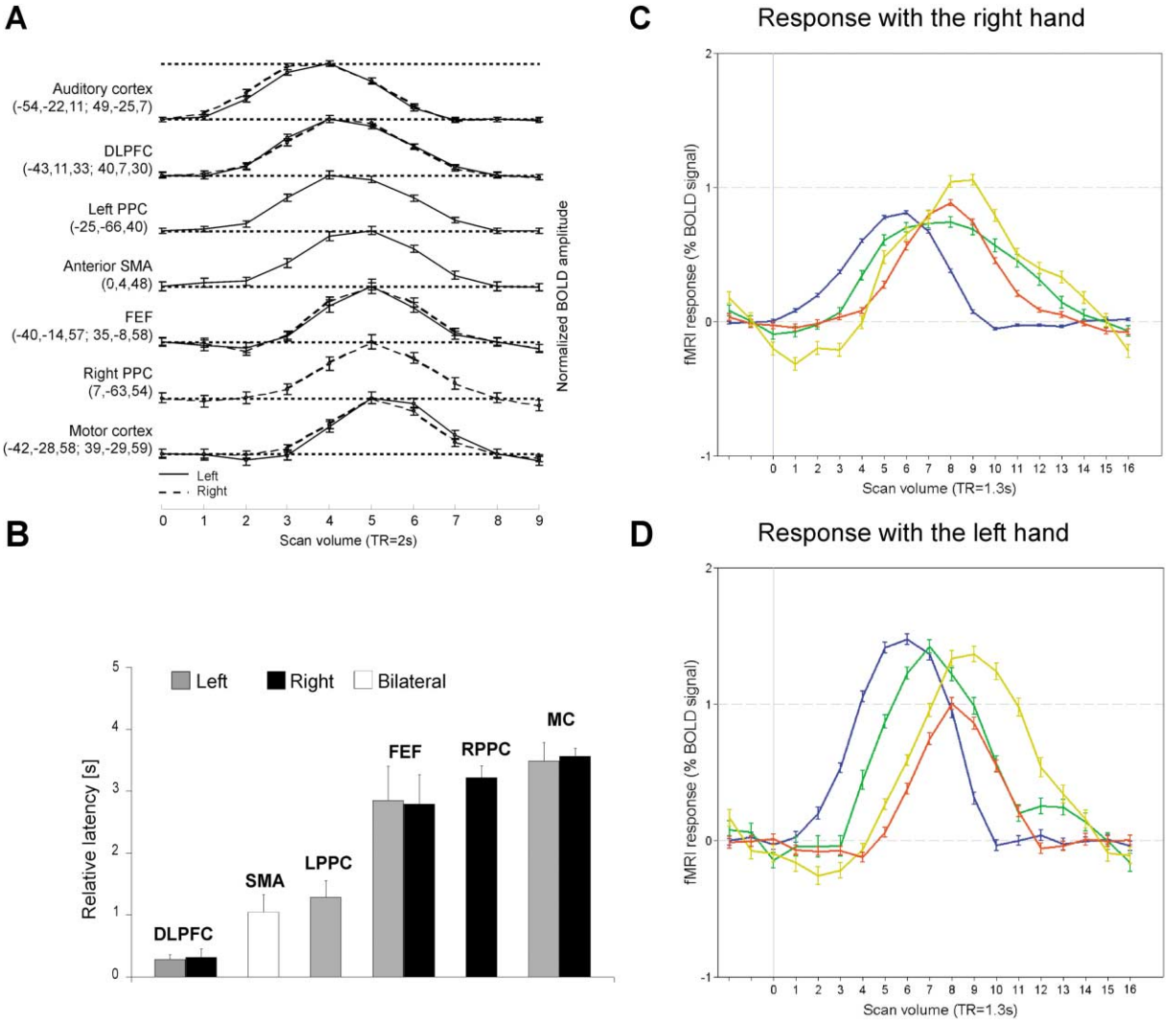

Figure 2. Event-Related Time Course Analysis

Grand-average time courses of the BOLD responses of significantly activated regions. Grand-average time courses were obtained by averaging the event-related responses of all the subjects ($n_1 = 6$, TR = 2 s). Error bars indicate one standard error of the mean. The Talairach coordinates of the center of mass of the activation clusters are indicated in brackets. (B) Mean relative latencies of the BOLD responses of significantly activated regions. For each of the six subjects, the relative latency of each region was computed as the difference between the onset time of the event-related averaged (64 trials) response of the region and the onset time of the event-related averaged response in the auditory cortex. Bars indicate the mean values of individual relative latencies. Error bars indicate one standard error of the mean. One-way ANOVA and post hoc Fisher tests were applied to relative latencies, in order to characterize significant temporal differences. The statistical analysis showed a robust effect of region (F [8,45]: 13.83; $p < 10^{-9}$) and the post hoc tests showed a significant difference ($p = 0.002$, corrected) between the relative latency of the left (1.28 $\pm$ 0.39 s) and the right (3.21 $\pm$ 0.27 s) posterior parietal cortex (Figure 2B). The same statistical analysis applied to amplitudes of hemodynamic responses showed no significant effect. (C and D) Event-related BOLD responses of the auditory cortex (blue), left (green) and right (yellow) posterior parietal cortex, and motor cortex (red) in a second group of subjects ($n_2 = 6$, TR = 1.3). Responses were averaged across the subjects that used the right ($n_{2R} = 3$, C) or the left hand ($n_{2L} = 3$, D) for the button press. AC = auditory cortex, DLPFC = dorso-lateral prefrontal cortex, FEF = frontal eye fields, LPPC = left posterior parietal cortex, MC = motor cortex, RPPC = right posterior parietal cortex, SMA = supplementary motor area.

effects on the described spatio-temporal pattern of activation were observed when trials were split according to the visual hemifield that corresponded to the position of the imagined clock hands (left and right) and analyzed separately.

Trial-by-Trial Analysis of Hemodynamic Responses and Correlation with Reaction Times

To test the hypothesis that the observed latency difference of HRs in separate cortical regions reflected their involvement in distinct processing stages of the mental clock task, we performed an analysis of trial-by-trial differences in the HRs and how these changes depended upon reaction times. For all the activated regions showing a significant effect in the first conventional analysis, the amplitude, the width, and the onset of the HRs to single trials of the task were estimated (see Experimental Procedures) and the correlations with RTs were calculated (Table 3). It is important to note that the reaction times did not enter as explanatory

Table 2. Significance of Latency Differences between BOLD Responses of the Selected Regions of Interest

	Left DLPFC	Right DLPFC	Left PPC	Anterior SMA	Left FEF	Right FEF	Right PPC	Left MC	Right MC
Left DLPFC	–								
Right DLPFC	>0.1	–							
Left PPC	0.06	>0.1	–						
Anterior SMA	>0.1	>0.1	>0.1	–					
Left FEF	*10^{-5}*	*10^{-5}*	*0.005*	*0.001*	–				
Right FEF	*10^{-5}*	*10^{-5}*	*0.008*	*0.002*	>0.1	–			
Right PPC	*10^{-6}*	*10^{-6}*	*0.002*	*10^{-4}*	>0.1	>0.1	–		
Left MC	*10^{-7}*	*10^{-7}*	*10^{-5}*	*10^{-5}*	>0.1	>0.1	>0.1	–	
Right MC	*10^{-8}*	*10^{-7}*	*10^{-5}*	*10^{-6}*	0.07	*0.05*	>0.1	>0.1	–

Post hoc Fisher tests were applied to relative latencies (see Figure 2B) of BOLD responses. Significant values ($p < 0.05$, corrected) are reported in italics.

variables into the first analysis and therefore this selection of regions did not bias the inferences about correlations with reaction times that are reported below.

In the auditory cortex and in the planum temporale, none of the parameters was significantly correlated with the RTs. The signal increase in these regions reflects the

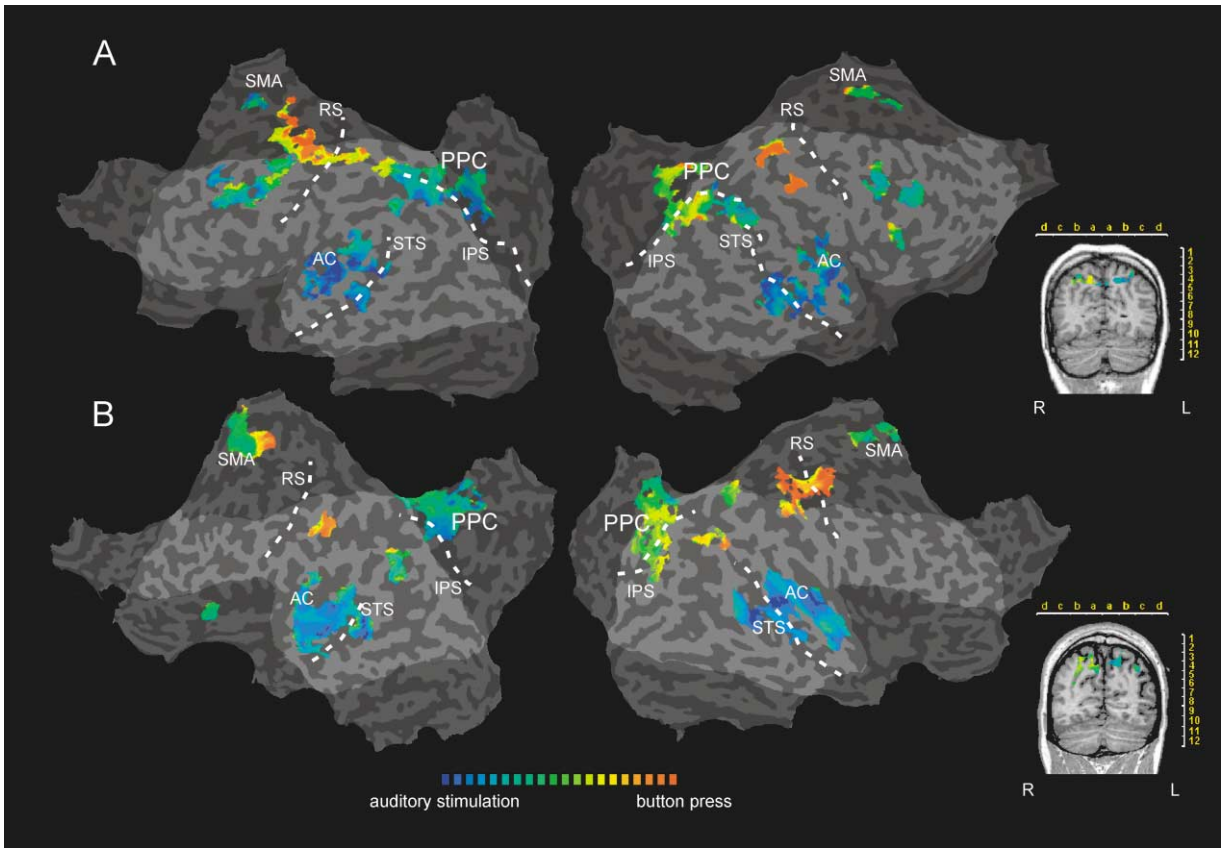

Figure 3. Cortex-Based Multiple Regression Analysis of fMRI Time Series: Individual Results

Individual general linear model surface map superimposed on flattened representation of the subject's cortex in a case of response with the right ([A], subject BS, TR = 2 s) and with the left ([B], subject VV, TR = 1.3 s) hand. Color code is the same as in Figure 1. Note the different degree of lateralization of early (blue-green) and late (yellow) activation in the left and right posterior parietal cortex. Inserts show the parietal activation superimposed on selected anatomical coronal slices ($y_A = -68$, and $y_B = -64$) in standard Talaraich space.

Left (right) flattened hemispheres are displayed on the left (right) side of the image. In the inserts, the left side of the image corresponds to the right side of the brain (radiological convention).

AC = auditory cortex, IPS = intraparietal sulcus (posterior branch), PPC = posterior parietal cortex, RS = rolandic sulcus, SMA = supplementary motor area, STS = superior temporal sulcus.

Table 3. Correlation between Reaction Times and Estimated Parameters (Onset, Width, and Amplitude) of the Hemodynamic Responses to Single Trials of the Mental Clock Task

		Onset		Width		Amplitude	
	No. of trials	Corr. with RTs	p	Corr. with RTs	p	Corr. with RTs	p
Auditory cortex	255	0.01	>0.1	−0.04	>0.1	0.01	>0.1
Left DLPFC	214	−0.04	>0.1	0.15	*0.03*	0.07	>0.1
Right DLPFC	263	0.05	>0.1	0.14	*0.02*	−0.07	>0.1
Left PPC	238	−0.10	>0.1	0.29	10^{-5}	0.15	*0.02*
Anterior SMA	282	0.07	>0.1	0.17	10^{-3}	0.13	*0.03*
Left FEF	215	0.04	>0.1	0.10	>0.1	−0.03	>0.1
Right FEF	207	0.01	>0.1	0.11	>0.1	0.01	>0.1
Right PPC	253	0.22	10^{-4}	−0.04	>0.1	0.11	0.09
Left MC	131	0.39	10^{-6}	0.01	>0.1	0.09	>0.1
Right MC	123	0.42	10^{-6}	−0.02	>0.1	0.10	>0.1

Significant values ($p < 0.05$) are shown in italics. No. of trials indicates the number of trials in which the parameters of the hemodynamic response could be estimated correctly by the fitting procedure (see Experimental Procedures).

processing of the acoustic stimuli, which had constant duration in all the trials. In the sensorimotor cortex, only onset of the HR, but neither amplitude nor width, showed a significant correlation with RT. This reflects the dependence of the BOLD responses in these regions on the timing of the button press responses. In the bilateral network of fronto-parietal regions that was activated during the task, we observed two different patterns of correlations. First, in the anterior SMA, the DLPFC, and the left PPC, onset of the HR was early and not correlated with RT, suggesting that the contribution of these regions starts in the early processing stages of the task. Furthermore, the width in these three regions was significantly correlated with RT (Table 3 and Figure 4). Secondly, in the right PPC (yellow clusters in Figures 1), onset of the HR was late and significantly correlated with RT (Table 3 and Figure 4), suggesting the involvement of this region in the late processing stages of the task.

Discussion

Our observation of the sequential activation of specialized brain regions during the mental clock task confirms the feasibility of performing mental chronometry of human brain functions with time-resolved, whole-brain fMRI. This method enabled us to address functional questions, in particular the issue of hemispheric specialization in the cortical system that subserves the generation and analysis of mental images.

We could trace both the topography and the sequence of cortical activation from auditory perception to motor response and identify a bilateral network of fronto-parietal regions that showed task-related activation. Coactivation of subsets of this fronto-parietal network has been reported in numerous studies of related cognitive or sensorimotor functions such as spatial and nonspatial attention (Wojciulik and Kanwisher, 1999; Kanwisher and Wojciulik, 2000), attention orienting and target detection (Corbetta et al., 2000; Linden et al., 1999), eye movements (Corbetta et al., 1998), and maintenance and manipulation of information during spatial and nonspatial working memory tasks (Cohen et al., 1997; LaBar et al., 1999; Smith and Jonides, 1999; Rowe et al., 2000). The common cognitive requirements shared by the tasks used in these studies and our imagery task might account for the overlap of activation patterns (Culham and Kanwisher, 2001). The activation of the FEFs that occurred after that of the remainder of the DLPFC (Figures 1 and 3) and at about the same time as that of the right PPC was probably related to the covert attention shifts (Corbetta et al., 1998; Goebel et al., 1998) required for the angle comparison in the last phase of the task.

The relatively early activation of the anterior supplementary motor area (SMA) (Figures 1 and 3) might reflect its role in semantic processing (Chee et al., 1999). Alternatively, it could be related to the function of this area in task sequencing and integration of multiple features in working memory (Munk et al., 2002). The later activation of the posterior SMA that was observed in individual maps (Figure 3) might be more closely related to the preparation of the motor response.

In the parietal lobes, activation was most prominent along the superior part of the IPS and in the superior parietal lobule (SPL). Activation of similar parietal regions has been reported as being very robust in a recent fMRI study of visuospatial mental imagery (Knauff et al., 2000). In other functional neuroimaging studies of visual imagery, a superior parietal activation has been reported in all those cases where the stimulation protocol required the spatial analysis of the imagined material (Cohen et al., 1996; Kosslyn et al., 1997; Mellet et al., 2000). In a recent fMRI study (Trojano et al., 2000), we addressed the specificity of this activation for mental imagery. The activation during the mental clock task (*imagery*) was compared with that evoked by the same operation performed on visually presented material (*perception*) and by a nonimagery control task, whose difficulty was comparable to that of the imagery task. This allowed us to fractionate the cognitive processes during the mental clock task and to demonstrate the involvement of bilateral areas located on the superior part of the IPS in the generation and spatial analysis of imagined objects. The comparison between the *imagery* and the *perception* conditions showed that the same areas were also activated during the spatial transformation of visual percepts, providing evidence for a specific convergence of the pathways of imagery and visual perception within the parietal lobes.

The analysis of the sequence of activated areas, which

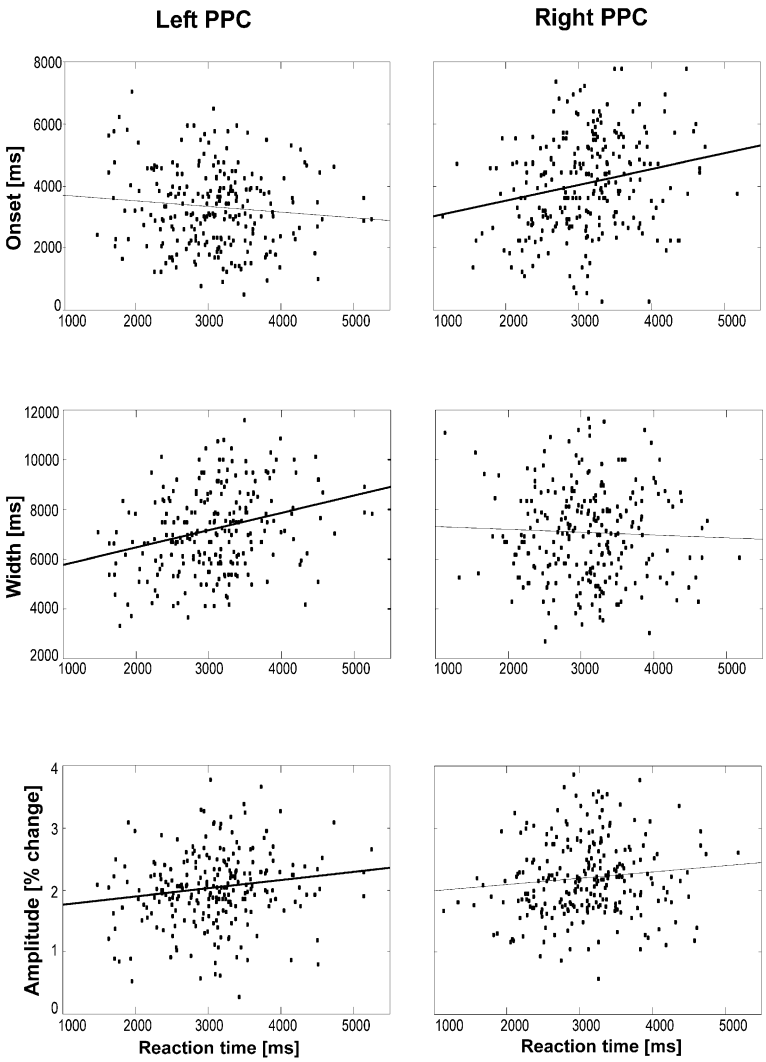

Figure 4. Correlation between Reaction Times and Parameters of the Hemodynamic Responses in the Posterior Parietal Cortex

Estimated values of onset, width, and amplitude (see Experimental Procedures) of the hemodynamic responses to single trials of the mental clock task in the left and right posterior parietal cortex (PPC) are plotted against the corresponding RTs. Bold lines indicate significant ($p < 0.05$) linear correlation. Note the complementary patterns of significant correlations in left and right PPC.

was made possible by the event-related design of the present study, revealed a temporal asymmetry of the activation in the left and right parietal lobes. While the left PPC was activated relatively early in the course of task performance, the main clusters of right PPC activity became active significantly later. Yet part of the right PPC also participated in earlier activation (see Figures 1 and 3), pointing to a transition from an early more distributed processing stage to a later stage that was largely confined to the right PPC. The implication that the sequence of activated clusters reflects a true sequence of processing stages, where subsequent operations depend on the results of previous operations, rather than local differences in the physiological mechanisms underlying the BOLD signal is further supported by the consideration that neurovascular coupling is likely to be governed by the same time constants in largely homologous anatomical regions and by the trial-by-trial analysis of BOLD responses (Figure 4). Whereas the sequence of activation of clusters in the left and right PPC strongly suggests separate functions for these regions, it is a matter of interpretation at this stage what their specific functional role might be. The task requires the subjects first to construct the multipart mental images of the clock faces, and then to inspect the constructed images in order to compare the angles formed by the hands. An interpretation that is compatible with the sequence of activation found in the present study would be that the early parietal activation, mainly but not exclusively confined to the left hemisphere, is specific to the construction of the mental image while the late activation of the right PPC reflects its subsequent inspection. The maintenance and manipulation of the information needed to construct the mental images might explain the mainly early activation of the frontal regions of the network (Trojano et al., 2000).

The behavioral data (Table 1) provide additional evidence for this interpretation. Subjects were faster when using their *left* hand to respond and when the clock hands to be imagined were in the *right* hemifield. Under the assumption that cross-callosal transfer of information causes additional costs in processing time, a functional dissociation in the PPC with the activation mainly located in the left hemisphere reflecting the construction of the multipart mental image and the activation in the right hemisphere reflecting the angle comparison would

lead to a benefit for imagery of objects in the right hemifield and for a left hand response. The analysis of the correlations of the parameters of the BOLD response with behavior also points to such a functional differentiation between left and right PPC. In the left PPC, only width and amplitude but not the onset of the evoked BOLD response correlated significantly with reaction times. This suggests that, while the duration of the left PPC process determined the subsequent processes of the task, it did not depend on previous processes of variable length itself. This could apply to the image generation process, which starts immediately after stimulus presentation and whose duration determines the onset of the spatial matching process. Similar correlations were observed in the DLPFC and anterior SMA, which might indicate that these areas cooperate in the construction of the mental image (working memory, sequencing). Conversely, in the right PPC, only the onset of the hemodynamic response correlated with reaction times. This points to a process that depends on the completion of an earlier process but itself has a constant duration. The spatial matching of the imagined clocks might be such a process.

These considerations, while consistent with the results of lesion studies, which show that a selective impairment of image generation is highly likely to be associated with left posterior lesions (Grossi et al., 1989; Farah et al., 1988; Trojano and Grossi, 1994; Stangalino et al., 1995; but see also Sergent, 1990; Kosslyn et al., 1995), would support the hypothesis of a "weak" left hemispheric lateralization for image generation (Farah, 1995). Furthermore, they would confirm the superiority of the right hemisphere in performing spatial analysis in imagery and nonimagery tasks. While our earlier study (Trojano et al., 2000) provided evidence for the convergence of visuospatial perceptual and imagery-related processes at the level of the PPC bilaterally, the present study suggests a special role of the left PPC in forming an explicit representation of the angular information for the purpose of a subsequent metric judgment. This cognitive process is required both when the clock faces are mentally generated and when they are visually perceived. A future time-resolved fMRI study with visually presented clocks might clarify whether the observed functional asymmetry also applies to the visual domain or is imagery specific.

In conclusion, this event-related fMRI study reveals the spatio-temporal dynamics of the sensory, cognitive, and motor processes underlying the execution of the mental clock task. While the spatial pattern of brain activation is in agreement with previous knowledge about the cortical processes related to visuospatial imagery, the temporal analysis of the brain activation highlighted an asymmetric pattern of functional responses in the left and right PPC. This functional asymmetry has been detected by group, individual, and single-trial analyses (Figures 1–4) and can explain the observed patterns of reaction times (Tables 1 and 3). These findings go beyond the identification of coactivated brain regions during a complex task and provide neurophysiologcial constraints for models of sequential information processing and lateralization in the human brain.

Experimental Procedures

Subjects

Twelve healthy right-handed subjects (7 male, 5 female; mean age 25.9 years; range 22–38) gave their informed consent and participated in the study. All of them were unaware of the purposes and predictions of the experiment at the time of testing.

Stimuli and Task

Stimuli were pairs of times, involving only half hours (e.g., 7.30) or full hours (e.g., 9.00), balanced for correspondence to numerically greater or smaller times (e.g., $3.00 > 1.00$) and for the visual hemifield that corresponded to the position of the imagined clock hands (e.g., right hemifield: 3.00 and 5.30, left hemifield: 9.00 and 7.00). Stimuli were digitized and presented in pseudorandom order using a custom-made MR-compatible auditory stimulation device (Dierks et al., 1999). Before starting the scanning session, subjects were familiarized with the material and the task. The instruction phase included a visual presentation of simplified clock faces and several practice trials. Subjects were instructed to imagine analog clock faces based on acoustically presented pairs of times and push a button with their index finger if the hands of the first clock formed the greater acute angle or another button with their middle finger if the hands of the second clock formed the greater acute angle. Subjects were asked to keep their eyes open during the scanning session and their eye position steady to a central fixation point. Subjects' responses were registered by an optic fiber answer box and analyzed for speed and accuracy.

Functional Imaging Data

The MR scanner used for imaging was a 1.5 T whole-body superconducting system (MAGNETOM Vision, Siemens Medical Systems, Erlangen, Germany) equipped with a standard head coil and an actively shielded gradient coil (25 mT/m). In a first group of subjects ($n_1 = 6$, 3 males, 3 females; mean age 24 years; range 22–26), a BOLD-sensitive single shot EPI sequence (Echo Time (TE) = 60 ms; Flip Angle (FA) = 90°; matrix size = 64×64, Voxel dimensions = $2.8 \times 2.8 \times 5$ mm^3) examining the whole brain with 16 slices in 2 s (TR = 2 s) was used for functional imaging. Each of these subjects performed an overall number of 64 trials of the mental clock task during four fMRI runs (16 trials per run, intertrial interval = 16 s) of 256 s (128 scans) each. Before each functional run, an external auditory cue informed the subjects to change the hand used for the button press response according to an A-B-B-A design. Both the group analysis of functional imaging and behavioral data were based on this first group of subjects. In a second group of subjects ($n_2 = 6$, 3 males, 3 females; mean age 27.8 years; range 24–38), functional time series were collected using a shorter TR (= 1.3 s; TE = 60 ms) and a smaller number of slices (= 10; voxel size = $3.13 \times 3.13 \times 7$ mm^3, interslice gap = 0.7 mm). In this case, subjects performed 23 trials (intertrial interval = 20.8s) of the clock task during an fMRI run of 520 s (400 scans). Half of these subjects used the left hand ($n_{2L} = 3$) and the other half the right hand ($n_{2R} = 3$) for the button press response. Data from these subjects were used to confirm the main finding of sequential activation of left and right PPC at a higher sampling rate (Figures 2C, 2D, and 3B). These data also served in a correlated repetitive transcranial magnetic stimulation study of mental imagery (see Sack et al., 2002) to investigate the relative position between clusters of functional activation and the locations of the TMS coil. For each subject, three-dimensional anatomical volumes were collected with a T1-weighted 3D MP-RAGE sequence (Magnetization-Prepared Rapid Acquisition Gradient Echo, TR = 9.7 ms, TE = 4 ms, FA = 12°, matrix = 256×256, thickness = 1 mm, number of partitions = 170–180, voxel dimensions = $1 \times 1 \times 1$ mm^3).

Data Analysis

Anatomical and functional images were analyzed using BrainVoyager 2000 (Brain Innovation, Maastricht, The Netherlands). Cortical surface reconstruction and flattening, functional time series preprocessing, including 3D motion correction, interscan slice time correction, gaussian spatial filtering (FWHM = 2 voxels), temporal filtering (removal of low-frequency drifts), transformation into Talairach

space (Talairach and Tournoux, 1988), and the generation of 4D functional time series (volume time course: 3 × space, 1 × time) followed procedures described elsewhere (Goebel et al., 2001; Dierks et al., 1999; Trojano et al., 2000; Kriegeskorte and Goebel, 2001).

Statistical analysis of 4D functional time series included both multi- and single-subject cortex-based multiple regression analysis. In the multi-subject analysis, the general linear model (GLM) of the experiment was computed from the z-normalized volume time courses ($n_1 = 6$, 4 runs per subject, TR = 2 s). In the single-subject analysis, the GLM was computed from the preprocessed individual volume time courses. In both cases, the signal values following the stimulus presentation were considered the effects of interest. Three predictors, defined to represent the auditory instruction, the mental imagery, and the motor response, were used to build the design matrix of the experiment. The first predictor was obtained using a model of the hemodynamic response (Boynton et al., 1996) to the auditory instruction, the other predictors by shifting this model by one or two bins of 2 s, respectively. The global level of the signal time courses in each session was considered as a confounding effect. The overall model fit was assessed using an F statistic. The obtained p values were corrected for multiple comparisons using a cortex-based Bonferroni adjustment, i.e., the number of comparisons considered was reduced by limiting the analysis to gray matter voxels (Trojano et al., 2000). Effects were only accepted as significant when p (corrected) $< 10^{-3}$. This very conservative threshold was selected to counterbalance the effect of the reduction of degrees of freedom resulting from the temporal filtering and to ensure robustness against violations of assumed sphericity amongst the error terms in the data.

For both group and individual analysis, the spatio-temporal pattern of activation was visualized using maps of relative latency. For each significantly activated voxel, the onset latency was estimated and color coded according to a blue-green-yellow-red scale (Figures 1 and 3). The onset latency was calculated as the time (measured from the stimulus onset) at which the estimated time course (i.e., the least square fit of the time course as resulting from the GLM) reached 10% of its peak value. The time interval between the minimum and the maximum values of the onset latencies was subdivided in twenty bins, with each bin corresponding to a color. The minimum latency of activation (auditory cortex) corresponded to the blue color; the maximum latency (motor cortex) corresponded to the red color. Intermediate values of onset latency were linearly scaled between these two extremes. Maps of relative latency were projected on inflated and flattened representations of the cortical sheet of a template brain (courtesy of the Montreal Neurological Institute) (group map) or of the subject's brain (individual maps).

Correlation between BOLD Responses and Reaction Times

In order to investigate the relations between the spatio-temporal pattern of activation and the subjects' RT, an additional trial-by-trial analysis of the BOLD responses was performed. For each significantly activated region and for each subject (n = 6, TR = 2 s), the BOLD response were selected, baseline-corrected, and interpolated to 1 s temporal resolution using spline interpolation. Onset, width, and amplitude of the responses were approximated by a minimum mean square error fitting with a set of trapezoids as described in Richter et al. (2000). BOLD responses corresponding to subjects' errors in performing the task as well as those that could not be fitted well (e.g., because of baseline drifts or other artifacts) were discarded. Each parameter (onset time, width, and amplitude) was correlated with RT.

Acknowledgments

The authors are grateful to Nikolaus Kriegeskorte, Bernadette Schmitt, Lars Muckli, and to the reviewers for useful comments on the manuscript.

Received: November 14, 2001
Revised: April 15, 2002

References

Boynton, G.M., Engel, S.A., Glover, G.H., and Heeger, D.J. (1996). Linear systems analysis of functional magnetic resonance imaging in human V1. J. Neurosci. *16*, 4207–4241.

Chee, M.W., O'Craven, K.M., Bergida, R., Rosen, B.R., and Savoy, R.L. (1999). Auditory and visual word processing studied with fMRI. Hum. Brain Mapp. *7*, 15–28.

Cohen, M.S., Kosslyn, S.M., Breiter, H.C., DiGirolamo, G.J., Thompson, W.L., Anderson, A.K., Brookheimer, S.Y., Rosen, B.R., and Belliveau, J.W. (1996). Changes in cortical activity during mental rotation. A mapping study using functional MRI. Brain *119*, 89–100.

Cohen, J.D., Perlstein, W.M., Braver, T.S., Nystrom, L.E., Noll, D.C., Jonides, J., and Smith, E.E. (1997). Temporal dynamics of brain activation during a working memory task. Nature *10*, 604–608.

Corbetta, M., Akbudak, E., Conturo, T.E., Snyder, A.Z., Ollinger, J.M., Drury, H.A., Linenweber, M.R., Petersen, S.E., Raichle, M.E., Van Essen, D.C., and Shulman, G.L. (1998). A common network of functional areas for attention and eye movements. Neuron *21*, 761–773.

Corbetta, M., Kincade, J.M., Ollinger, J.M., McAvoy, M.P., and Shulman, G.L. (2000). Voluntary orienting is dissociated from target detection in human posterior parietal cortex. Nat. Neurosci. *3*, 292–297.

Culham, J.C., and Kanwisher, N.G. (2001). Neuroimaging of cognitive functions in human parietal cortex. Curr. Opin. Neurobiol. *11*, 157–163.

Dierks, T., Linden, D.E.J., Jandl, M., Formisano, E., Goebel, R., Lanfermann, H., and Singer, W. (1999). Activation of Heschl's gyrus during auditory hallucinations. Neuron *22*, 615–621.

Farah, M.J. (1995). Current issues in the neuropsychology of image generation. Neuropsychologia *33*, 1455–1471.

Farah, M.J., Levine, D.N., and Calvanio, R. (1988). A case study of mental imagery deficit. Brain Cogn. *8*, 147–164.

Friston, K.J., Holmes, A.P., Worsley, K.J., Poline, J.P., Frith, C.D., and Frackowiak, R.S.J. (1995). Statistical parametric maps in functional imaging: a general linear approach. Hum. Brain Mapp. *2*, 189–210.

Goebel, R., Linden, D.E.J., Lanfermann, H., Zanella, F.E., and Singer, W. (1998). Functional imaging of mirror and inverse reading reveals separate coactivated networks for oculomotion and spatial transformations. Neuroreport *9*, 713–719.

Goebel, R., Muckli, L., Zanella, F.E., Singer, W., and Stoerig, P. (2001). Sustained extrastriate cortical activation without visual awareness revealed by fMRI studies of hemianopic patients. Vision Res. *41*, 1459–1474.

Grossi, D., Modafferi, A., Pelosi, L., and Trojano, L. (1989). On the different roles of the two cerebral hemispheres in mental imagery: the "O'Clock test" in two clinical cases. Brain Cogn. *10*, 18–27.

Hillyard, S.A. (1993). Electrical and magnetic brain recordings: contributions to cognitive neuroscience. Curr. Opin. Neurobiol. *3*, 217–224.

Kanwisher, N., and Wojciulik, E. (2000). Visual attention: insights from brain imaging. Nat. Rev. Neurosci. *1*, 91–100.

Knauff, M., Kassubek, J., Mulack, T., and Greenlee, M.W. (2000). Cortical activation evoked by visual mental imagery as measured by fMRI. Neuroreport *11*, 3957–3962.

Kosslyn, S.M. (1994). Image and brain: the resolution of the imagery debate (Cambridge, MA: MIT Press).

Kosslyn, S.M., Maljkovic, V., Hamilton, S.E., Horwitz, G., and Thompson, W.L. (1995). Two types of image generation: evidence for left and right hemisphere processes. Neuropsychologia *33*, 1485–1510.

Kosslyn, S.M., Thompson, W.L., and Alpert, N.M. (1997). Neural systems shared by visual imagery and visual perception: a positron emission tomography study. Neuroimage *6*, 320–334.

Kriegeskorte, N., and Goebel, R. (2001). An efficient algorithm for topologically correct segmentation of the cortical sheet in anatomical MR volumes. Neuroimage *14*, 329–346.

LaBar, K.S., Gitelman, D.R., Parrish, T.B., and Mesulam, M. (1999). Neuroanatomic overlap of working memory and spatial attention networks: a functional MRI comparison within subjects. Neuroimage *10*, 695–704.

Linden, D.E.J., Prvulovic, D., Formisano, E., Völlinger, M., Zanella, F.E., Goebel, R., and Dierks, T. (1999). The functional neuroanatomy of target detection: an fMRI study of visual and auditory oddball tasks. Cereb. Cortex *9*, 815–823.

Mellet, E., Tzourio-Mazoyer, N., Bricogne, S., Mazoyer, B., Kosslyn, S.M., and Denis, M. (2000). Functional anatomy of high-resolution visual mental imagery. J. Cogn. Neurosci. *12*, 98–109.

Menon, R.S., and Kim, S.-G. (1999). Spatial and temporal limits in cognitive neuroimaging with fMRI. Trends Cogn. Sci. *3*, 207–216.

Menon, R.S., Luknowsky, D.C., and Gati, J.S. (1998). Mental chronometry using latency-resolved functional MRI. Proc. Natl. Acad. Sci. USA *95*, 10902–10907.

Munk, M.H.J., Linden, D.E.J., Muckli, L., Lanfermann, H., Zanella, F.E., Singer, W., and Goebel, R. (2002). Distributed cortical systems in visual short-term memory revealed by event-related functional magnetic resonance imaging. Cereb. Cortex, in press.

Paivio, A. (1978). Comparisons of mental clocks. J. Exp. Psychol. Hum. Percept. Perform. *4*, 61–71.

Posner, M.I. (1978). Chronometric exploration of mind (London: Oxford University Press).

Raij, T. (1999). Patterns of brain activity during visual imagery of letters. J. Cogn. Neurosci. *11*, 282–299.

Renault, B., Ragot, R., Lesevre, N., and Remond, A. (1982). Onset and offset of brain events as indices of mental chronometry. Science *215*, 1413–1415.

Richter, W., Somorjai, R., Summers, R., Jarmasz, M., Menon, R.S., Gati, J.S., Georgopoulos, A.P., Tegeler, C., Ugurbil, K., and Kim, S.G. (2000). Motor area activity during mental rotation studied by time-resolved single-trial fMRI. J. Cogn. Neurosci. *12*, 310–320.

Rowe, J.B., Toni, I., Josephs, O., Frackowiak, R.S., and Passingham, R.E. (2000). The prefrontal cortex: response selection or maintenance within working memory? Science *288*, 1656–1660.

Sack, A.T., Sperling, J.M., Prvulovic, D., Formisano, E., Goebel, R., Di Salle, F., Dierks, T., and Linden, D.E.J. (2002). Tracking the mind's image in the brain II: transcranial magnetic stimulation reveals parietal asymmetry in visuospatial imagery. Neuron *35*, this issue, 195–204.

Sergent, J. (1990). The neuropsychology of visual image generation: data, method, theory. Brain Cogn. *13*, 98–129.

Shepard, R.N., and Cooper, L.A. (1982). Mental images and their transformation (Cambridge, MA: MIT Press).

Smith, E.E., and Jonides, J. (1999). Storage and executive processes in the frontal lobes. Science *283*, 1657–1661.

Stangalino, C., Semenza, C., and Mondini, S. (1995). Generating visual mental imagery: deficit after brain damage. Neuropsychologia *33*, 1473–1483.

Talairach, J., and Tournoux, P. (1988). Co-planar stereotaxic atlas of the human brain (Stuttgart: G. Thieme).

Trojano, L., and Grossi, D. (1994). A critical review of mental imagery defects. Brain Cogn. *24*, 213–243.

Trojano, L., Grossi, D., Linden, D.E.J., Formisano, E., Hacker, H., Zanella, F.E., Goebel, R., and Di Salle, F. (2000). Matching two imagined clocks: the functional anatomy of spatial analysis in the absence of visual stimulation. Cereb. Cortex *10*, 473–481.

Wojciulik, E., and Kanwisher, N. (1999). The generality of parietal involvement in visual attention. Neuron *23*, 747–764.